Agricultural Water Management 289 (2023) 108556

Contents lists available at ScienceDirect

Agricultural Water Management

journal homepage: www.elsevier.com/locate/agwat

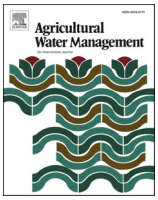

Performance of the Copernicus European Regional Reanalysis (CERRA) dataset as proxy of ground-based agrometeorological data

A. Pelosi

Department of Civil Engineering (DICIV) - University of Salerno, Italy

ARTICLE INFO

Handling Editor: Dr. Xiying Zhang

Keywords:
Reanalysis data
ERA5
ERA5-Land
Weather variables
FAO Penman-Monteith reference evapotranspiration
Mediterranean climate

ABSTRACT

The continuous advances in numerical modeling of the atmosphere, computing power and data assimilation techniques entail frequent updates of numerical weather prediction (NWP) models that show improved forecast skill. This circumstance leads to the recurrent delivery of revised reanalysis databases that provide weather estimates for several decades back in time by combining the latest NWP models with observations. Since climate studies and agriculture water management applications require the availability of accurate and reliable weather data, assessing the performance of reanalysis products contributes to informed choices of potential weather proxy of ground-based agrometeorological data. CERRA (Copernicus European Regional ReAnalysis) dataset is the latest regional reanalysis product released by the European Centre for Medium-Range Weather Forecasts (ECMWF), in August 2022. CERRA is forced by the global ERA5 reanalysis, and it provides weather data with resolution of 5.5 km for the pan-European territory from 1984. For the first time in literature, this study explores the performance of CERRA data at 38 ground-based weather stations located in Sicily, an Italian region with Mediterranean climate, during the irrigation seasons 2003–2022. The objective of the study lies in evaluating CERRA performance with respect to air temperature, actual vapor pressure, wind speed and solar radiation that are input variables for assessing reference evapotranspiration, ET_O, which is a key variable for quantifying irrigation volumes needed for water resources studies. The accuracy of ET_O estimates depends on those input variables through the equation provided by the Food and Agriculture Organization of the United Nations (FAO), i.e., the FAO Penman-Monteith equation. Here, it is also evaluated the performance of ET_O estimates by using CERRA weather inputs in the FAO Penman-Monteith equation. The results show that the performances of CERRA weather data are excellent, especially for air temperature, and this determines that CERRA ET_O estimates present high accuracy and reliability with a mean PBIAS and NRMSE equal to 5.6% and 13%, respectively, over the region. Those outcomes lead to the conclusion that CERRA dataset represents a valid alternative to ground-based agrometeorological measurements and their spatial interpolation for water resource regional studies.

1. Introduction

The increasing availability and quality of weather databases from different sources than ground-based monitoring networks, such as numerical modeling, may improve the assessment of hydrological variables for regional studies on agricultural water resources and management in data-sparse regions. Indeed, agricultural water management is strictly linked to the availability and quality of weather data at regional scale through the quantification of irrigation water use in a district that is essential for planning the allocation of water resources in agriculture and designing irrigation systems (Iglesias and Garrote, 2015; Pereira, 2017). Quantitative assessment of irrigation volumes is generally based on crop-water-balance models that need reference evapotranspiration, ET_O, as input data (e.g., Calera et al., 2017). ET_O can be interpreted as a synthetic index of the influence of weather conditions on crop evapotranspiration and crop water requirements (Allen, 2000) and, according to the most advanced method for its computation provided by the Food and Agriculture Organization of the United Nations (FAO), i.e., the FAO-56 Penman-Monteith equation, it depends on a complete set of agrometeorological data, such as air temperature, air relative humidity, wind speed and solar radiation (Allen et al., 1998). Those data are available at a limited number of sites in a region, according to the density of the ground-based monitoring networks that are usually sparse, even in developed countries (Pelosi et al., 2020a). The density of the monitoring networks severely impacts on the performance of the spatial interpolation techniques used for assessing weather data at

E-mail address: apelosi@unisa.it.

https://doi.org/10.1016/j.agwat.2023.108556
Received 4 June 2023; Received in revised form 10 October 2023; Accepted 12 October 2023
Available online 23 October 2023

ungauged sites as well as for creating gridded data over a region (Berndt and Haberlandt, 2018). Moreover, the observed time-series are often short, especially for variables like air relative humidity, wind speed and solar radiation.

In this context, different sources than ground-based agro-meteorological networks may be considered as a potential alternative to provide a set of gridded weather data that covers several decades back in time with high spatial resolution. Over the past 40 years, numerical weather prediction (NWP) models have undergone a "quiet revolution" (Bauer et al., 2015) due to the excellent scientific and technological developments that have led to increasing weather forecast skills. Thus, NWP model outputs have been used with excellent outcomes in many studies to support irrigation system operation and scheduling in the near real-time forecast mode (e.g., Perera et al., 2014; Pelosi et al., 2016; Chirico et al., 2018; Medina et al., 2018; Longo-Minnolo et al., 2020; Pelosi et al., 2020b; Vanella et al., 2020).

For climate studies, NWP models are let run back in time and constantly updated by sequentially assimilating ground and satellite-based weather observations to create reanalysis databases, which represent robust and continuous weather databases that are coherent from both physical and dynamic perspectives (Soci et al., 2016), with a given spatial resolution that depends on the NWP model used. Some of the main advantages of reanalysis data also rely on their gratuitousness and ease of access and use. In recent years, several studies have exploited reanalysis data as proxy of ground-based weather data for various agrometeorological applications and reference evapotranspiration assessment studies. These studies are available for different regions and countries over the entire globe for which the reanalysis data are released: for instance, some of the most representative studies that used reanalysis data for assessing ET_O regarded the United Kingdom (Srivastava et al., 2015), France (Boulard et al., 2016), Iberian Peninsula (e.g., Martins et al., 2017; Paredes et al., 2018), Italy (e.g., Pelosi et al., 2020a; Pelosi and Chirico, 2021; Vanella et al., 2022), Iran (Raziei and Parehkar, 2021; Nouri and Homaee, 2022), Turkey (Irvem and Ozbuldu, 2022), United States (e.g., Albano et al., 2022), South America (Merino and Gassmann, 2023), and China (e.g., Zhao and He, 2022; Yu et al., 2023). Moreover, these studies analyzed and, eventually, compared different reanalysis databases provided by different meteorological centers that constantly update their reanalysis databases as soon as more sophisticated and accurate NWP models are released.

Some of the earliest cited studies considered global reanalysis data provided by the National Center for Environmental Prediction/National Center for Atmospheric Research (NCEP/NCAR), named NCEP/NCAR Reanalysis (e.g., Srivastava et al., 2015; Martins et al., 2017), followed by Raziei and Parehkar (2021) who analyzed the more recent NCEP/NCAR-PrincUV outputs, and by other studies that focused on the alternative ERA-Interim global reanalysis released by the European Centre for Medium-Range Weather Forecasts, ECMWF (e.g., Boulard et al., 2016; Paredes et al., 2018).

The ECMWF, along with ERA-Interim global reanalysis that has a spatial resolution of about 79 km over Europe, issued regional and surface reanalyses specifically for Europe: UERRA HARMONIE and UERRA MESCAN-SURFEX (UMS). The latter dataset has a spatial resolution of 5.5 km, and its outputs were examined by Pelosi et al. (2020a) for the assessment of ET_O in Southern Italy. This study found that the performances of the regional database UERRA MESCAN-SURFEX were better than the ones of the native global reanalysis, ERA-Interim, as expected, since regional reanalysis represents a dynamical downscaling of the global dataset, forced by a high-resolution limited-area NWP model, and coupled with a regional data assimilation scheme to improve resolution and model outputs forecast skills (Cerenzia et al., 2022).

Currently, both ERA-Interim and UMS were outdated since, in 2019, the ECMWF released the fifth-generation reanalysis database for the global climate and weather, ERA5, available on a regular latitude-longitude grid of 0.25 degrees (about 31 km over Europe) from 1940 to the present (Hersbach et al., 2020). In addition, another global reanalysis database was issued by replaying the land component of the ERA5 climate reanalysis with a finer spatial resolution of about 9 km, called ERA5-Land (Muñoz, 2019).

An increasing interest in these newest databases, ERA5 and ERA5-Land, led to many recent studies that evaluated their outputs as proxy of agrometeorological data for the assessment of ET_O (e.g., Pelosi et al. (2020a); He, (2022); Merino and Gassmann, 2023). In addition, lately Pelosi et al. (2022) combined ERA5-Land data with Sentinel-2 satellite imagery for assessing crop water requirements and yield in Southern Italy. All cited studies found that both ERA5 and ERA5-Land show excellent performance for estimating weather variables such as air temperature, air relative humidity, solar radiation, and wind speed, especially for what concerns air temperature. Those outcomes also led to the conclusion that ET_O estimates by using reanalysis data as weather input are reliable and accurate. Moreover, Vanella et al. (2022) showed that ERA5-Land slightly outperforms ERA5, due to the higher resolution grid for which some variables were optimized. Pelosi et al. (2020a) showed that ERA5-Land data outperforms the regional outdated database UERRA MESCAN-SURFEX, despite the coarser numerical grid. This result testifies that the choice of the gridded product should be not merely driven by its nominal spatial resolution but by the NWP model forecast skill. Indeed, ERA5-Land benefits of the latest ERA5 global reanalysis, while UMS is instead a downscaled product of UERRA-HARMONIE regional reanalysis, whose boundary conditions were defined by the outdated ERA-Interim.

However, only in August 2022 the ECMWF regional reanalysis database, forced by the latest global ERA5 reanalysis, was released: the Copernicus European Regional ReAnalysis, CERRA (Schimanke et al., 2021). CERRA database was produced under the framework of the Copernicus Climate Change Service to support adaptation actions and policy development as well as contribute to climate services, climate monitoring and research (CERRA, 2022). CERRA intends to replace the former ECMWF regional reanalysis UERRA with a spatial resolution of 5.5 km. Currently, CERRA data extend from 1984 to present (near real time).

In this study, to our knowledge for the first time in literature, the performances of CERRA outputs were investigated and, specifically, for the weather variables needed to reference evapotranspiration estimates, such as air temperature, air relative humidity (for the computation of actual vapor pressure), solar radiation, and wind speed. Moreover, an analysis about the advantage of using CERRA weather data as proxy of agrometeorological data for the assessment of ET_O at regional scale was carried out in the fashion of previous studies. Sicily island located in Southern Italy was chosen as study area since it represents a typical environment in the Mediterranean area, and it was object of other similar studies related to ERA5-Land on the topic (Pelosi and Chirico, 2021).

The novelty of the study lies on using the most up-to-date ECMWF reanalysis products that should be considered at regional level as an alternative to the weather variables predicted by spatially interpolating ground-based weather data.

2. Study area and data

2.1. Study area and observed ground-based weather data

The study area was Sicily, an island located in southern Italy, having an extension of about 25,000 km^2. The area is characterized by a complex topography with elevations ranging from 0 m a.m.s.l. to about 3230 m a.m.s.l. The small islands surrounding the region were omitted from the present study. In Fig. 1, the location and relief map of the region are displayed along with the locations of the automatic weather stations (AWSs), belonging to the agrometeorological monitoring network managed by the Sicilian Agrometeorological Information Service (SIAS –*Servizio Informativo Agrometereologico Siciliano,* www.sias.regione.sicilia.it), whose ground-based weather data ranging from year

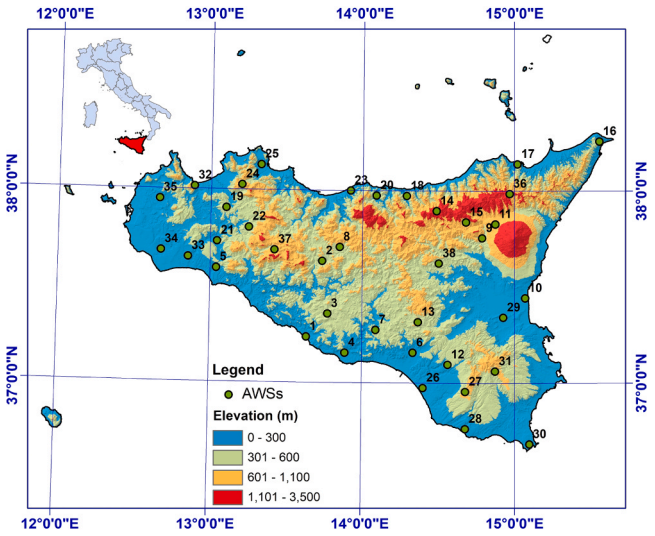

Fig. 1. Location and relief map of the study area along with the location of the 38 automatic weather stations (AWSs) used for the analysis (green circles) – the ID number of each AWS shown on the map is related to the name and climatic features of the station in Table 1.

2003 to 2022 were used in this study.

The climate of the study area is classified as hot dry-summer subtropical climate, also known as "typical Mediterranean climate," which, under the Köppen-Geiger climate classification, means (i) hot/very hot, dry summers that show minimum daily precipitation, frequently equal to 0 mm, and average daily mean air temperature close to 25 °C with daily peaks over 40 °C, and, (ii) mild, wet winters, which are characterized by maximum precipitation and minimum air temperature (Peel et al., 2007).

The climate of the region makes necessary open field irrigation in agriculture practices: field irrigation generally starts in April and lasts until the end of September, although the actual time span of the irrigation season is influenced by weather fluctuations and specific cropping practices. In the following, as done in previous studies related to this region and Southern Italy (i.e., Pelosi et al., 2016; Pelosi et al., 2020a), the period from April 1st to September 30th will be referred to as the irrigation season (183 days).

During the irrigation season, the spatial variability of the weather is strongly influenced by the month, topography, proximity of the Mediterranean Sea and latitude. Fig. 2 makes this clear, in terms of spatial variation of the monthly-averaged daily mean air temperature (Fig. 2a) and daily precipitation (Fig. 2b) in the six months belonging to the period of interest.

On April, the colder month in the analyzed period, the daily mean air temperature ranges from 7 °C to 17 °C, over the region, while on July, the hotter one, from 18 °C to 28 °C. Daily precipitation is on average almost zero from May to August and it still assumes negligible average values in the other months, up to 4 mm on average.

The lower temperatures are reached at higher elevations, especially in the mountainous area located in the north-eastern part of the region as well as in the eastern inner side of the island. On the coasts, especially in the south-western side, the weather may be affected by the African currents, so summers in such areas can often be very similar to summers of semi-arid climates (Pelosi and Chirico, 2021). Exceptional events of dust from Saharan Desert, carried by hot winds to Sicily and, in general, to southern Italy, may influence the weather of the region, especially in autumn and spring. However, the anomalous conditions due to Saharan dust usually last few days and do not show an increasing trend in both intensity and frequency over years (Pey et al., 2013). In the following, these events, and the resulting biases in the weather estimates from numerical modeling are treated only statistically, assuming that their duration and frequency are negligible for the purposes of the study. Moreover, any long-term trend in climate, which was recently documented in literature for the case of temperature (Liuzzo et al., 2017), was not here considered due to the focus of the study in the short-medium-term.

Specifically, the weather variables investigated in the following were daily aggregation of air temperature, wind speed, incoming shortwave solar radiation, and air relative humidity to estimate actual vapor pressure. Those data were, then, used as input variables to assess daily ET_O with the FAO-56 Penman-Monteith equation (Allen et al., 1998).

For a full description of the database as well as details about selection of AWSs and quality verifications (Allen, 1996), please refer to the study by Pelosi and Chirico (2021). Here, for the sake of completeness, Table 1 (Pelosi and Chirico, 2021) is reported to provide a list of the selected 38 AWSs used for this study, along with their geographic coordinates, elevation (ranging from 10 m a.s.m.l. to 1470 m a.s.m.l.) and weather data statistics recorded in the 20 seasons of interest (in years 2003–2022). The start dates of the data collection are also reported in Table 1: more than the 86% of the AWSs were installed before the irrigation season 2002; however, many gaps in the time series of year 2002 were found so that the analyses for the current study started on April 2003. For only the 8% of the AWSs, the measurements began later than April 2003: in the follows, for these stations the daily measurements from 2003 to the start of the data collection were considered as missing

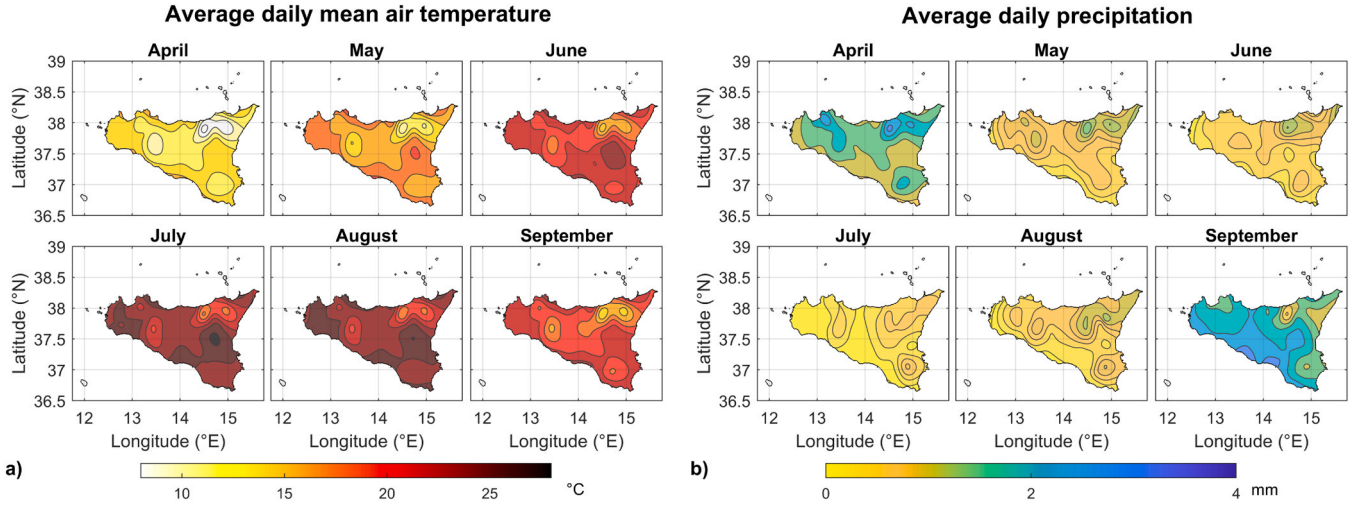

Fig. 2. Spatial variation over the region of the monthly-averaged a) daily mean air temperature and b) daily precipitation.

Table 1
Main statistics of the selected automatic weather stations in Sicily.

No.	Name	Start date of measurements	Elevation (m)	Longitude (°E)	Latitude (°N)	T_{max} (°C)	T_{min} (°C)	R_S (W m^{-2})	e_a (kPa)	$WS_{10\,m}$ (m s^{-1})
1	Agrigento	29/03/2002	40	13° 38' 09''	37° 14' 16''	26.2	16.8	275	1.6	2.9
2	Cammarata	29/01/2002	379	13° 44' 11''	37° 37' 55'	28.5	12.8	263	1.3	2.2
3	Canicattì	20/03/2002	475	13° 46' 24''	37° 21' 30''	27.7	14.1	260	1.3	2.1
4	Licata	01/01/2002	80	13° 53' 20''	37° 09' 20''	28.1	18.0	275	1.5	3.6
5	Sciacca	13/08/2002	90	13° 02' 23''	37° 35' 30''	28.6	17.0	278	1.4	2.9
6	Gela	25/02/2002	70	14° 20° 01''	37° 09' 32''	29.3	15.1	272	1.4	3.1
7	Riesi	29/01/2002	300	14° 05' 21''	37° 16' 32''	28.7	16.0	263	1.4	2.2
8	Sclafani Bagni	01/01/2002	497	13° 51' 00''	37° 42' 21''	28.0	13.0	267	1.2	1.6
9	Bronte	01/01/2002	424	14° 47' 13''	37° 45' 18''	29.1	13.7	251	1.2	1.5
10	Catania	01/01/2002	10	15° 04' 08''	37° 26' 26''	28.1	16.9	266	1.5	2.2
11	Maletto	01/01/2002	1040	14° 52' 23''	37° 49' 39''	23.3	13.4	252	1.1	2.1
12	Mazzarrone	01/01/2002	300	14° 33' 42''	37° 05' 45''	28.3	15.2	268	1.3	2.5
13	Piazza Armerina	18/01/2002	540	14° 21' 59''	37° 19' 02''	27.4	14.9	264	1.2	2.3
14	Caronia	21/09/2002	1470	14° 29' 11''	37° 53' 48''	17.9	10.2	255	1.0	3.8
15	Cesarò	25/01/2002	820	14° 40' 47''	37° 50' 19''	24.9	13.8	254	1.1	2.2
16	Messina	23/01/2002	420	15° 33' 40''	38° 15' 31''	23.5	16.7	263	1.6	3.8
17	Patti	02/03/2002	88	15° 01' 10''	38° 08' 28''	27.0	16.3	257	1.6	1.2
18	Pettineo	01/01/2002	210	14° 17' 00''	37° 58' 27''	26.4	17.3	259	1.5	2.1
19	Camporeale	01/01/2002	460	13° 06' 03''	37° 54' 18''	26.2	16.1	263	1.4	2.3
20	Castelbuono	01/01/2002	430	14° 05' 23''	37° 58' 29''	25.3	16.7	264	1.4	2.2
21	Contessa Entellina	11/02/2002	200	13° 02' 36''	37° 43' 50''	29.4	15.4	268	1.4	2.8
22	Corleone	02/01/2002	450	13° 15' 02''	37° 48' 17''	27.8	15.6	265	1.3	2.4
23	Lascari	16/02/2002	55	13° 55' 12''	38° 00' 00''	27.5	17.1	259	1.6	1.8
24	Monreale	01/02/2002	612	13° 12' 11''	38° 01' 32''	25.3	14.5	262	1.3	2.7
25	Palermo	01/01/2002	50	13° 19' 40''	38° 07' 51''	27.4	18.5	256	1.5	1.5
26	Acate	01/01/2002	60	14° 24' 02''	36° 58' 30''	27.2	16.7	272	1.8	2.2
27	Ragusa	01/01/2002	705	14° 40' 37''	36° 57' 20''	24.5	15.9	278	1.3	3.9
28	Scicli	01/01/2002	51	14° 40' 36''	36° 45' 40''	26.8	17.6	269	1.7	2.8
29	Lentini	25/01/2002	50	14° 55' 32''	37° 20' 32''	29.8	16.6	265	1.4	3.0
30	Pachino	04/01/2002	50	15° 05' 43''	36° 40' 57''	26.4	18.2	279	1.8	3.2
31	Palazzolo Acreide	13/01/2002	640	14° 52' 18''	37° 03' 43''	26.6	15.8	260	1.3	2.8
32	Castellammare del Golfo	01/01/2002	90	12° 53' 22''	38° 00' 52''	26.8	16.9	255	1.7	1.9
33	Castelvetrano	01/01/2002	120	12° 51' 10''	37° 38' 52''	28.2	15.6	271	1.4	2.7
34	Mazara del Vallo	01/01/2002	30	12° 40' 30''	37° 40' 47''	28.5	14.9	269	1.5	2.8
35	Trapani	23/02/2002	180	12° 39' 41''	37° 56' 51''	27.4	17.1	266	1.5	3.8
36	Montalbano Elicona	24/09/2004	1250	14° 58' 00''	37° 59' 10''	19.8	11.6	238	1.2	3.5
37	Prizzi	25/11/2004	1124	13° 25' 18''	37° 41' 20''	22.9	13.4	257	1.1	3.4
38	Agira	23/06/2006	467	14° 30' 07''	37° 37' 24''	28.3	16.3	262	1.2	2.9

data.

Then, Table 2 summarizes some average statistics of the data recorded from April to September updated for the 20 years of the present study (2003–2022). T_{max} (°C) and T_{min} (°C) are, respectively, the daily maximum and minimum air temperature measured at 2 m, R_S (W m^{-2}) is the daily mean of the incoming shortwave solar radiation, $WS_{10\,m}$ (m s^{-1}) is the daily mean of the wind speed measured at 10 m.

Regarding the daily mean actual vapor pressure, e_a (kPa), there are different formulations available for its computation that use different input data, such as daily mean dewpoint temperature or daily mean air relative humidity or daily maximum and minimum air relative humidity (Allen et al., 1998); here e_a was derived from the daily maximum and minimum air relative humidity measured at 2 m, RH_{max} (%) and RH_{min} (%) respectively, as follows (Allen et al., 1998):

$$e_a = \frac{e^0(T_{min})\frac{RH_{max}}{100} + e^0(T_{max})\frac{RH_{min}}{100}}{2} \quad (1)$$

Table 2
Regional mean statistics of the daily weather variables of interest, based on data collected during the 20 irrigation seasons examined (2003–2022).

	Mean	Coefficient of variation
T_{max}	27 °C	0.13
T_{min}	15 °C	0.18
R_S	268 W m^{-2}	0.21
e_a	1.4 kPa	0.19
$WS_{10\,m}$	2.6 m s^{-1}	0.36

where $e^0(T_{max})$ and $e^0(T_{min})$ are the saturation vapor pressures (kPa) computed at the daily maximum and minimum air temperatures, respectively. The relation between the saturation vapor pressure (kPa) and temperature (°C) is given by the following expression (Allen et al., 1998):

$$e^0(T) = 0.6108\exp\left[\frac{17.27T}{T+237.3}\right] \quad (2)$$

The analyses of the present study regard the evaluation of the newest weather data source CERRA as proxy of ground-based observed weather data, assumed as weather truth, for the assessment of daily reference evapotranspiration at regional scale in the irrigation seasons of the years 2003–2022. Details on the newest weather reanalysis database CERRA are given in the next section.

2.2. CERRA reanalysis data

Weather reanalysis optimally combines NWP model outputs that obey physical laws with ground- and satellite-based observations by data assimilation techniques (Soci et al., 2016; Pelosi et al., 2020a). The result of the data assimilation step that corrects the NWP outputs with observations is called the analysis: it represents the best estimate of the state of the atmosphere from which an updated, improved forecast is then issued by implementing the NWP model for the following time steps until the next assimilation (CERRA, 2022).

Weather reanalysis data employed in the present study belong to the Copernicus European Regional ReAnalysis (CERRA) dataset (Schimanke

et al., 2021), which is the latest reanalysis dataset freely released in August 2022 by the ECMWF on the Copernicus Climate Data Store (https://cds.climate.copernicus.eu).

CERRA is a regional reanalysis product whose input data are both weather observations for the assimilation steps and lateral boundary conditions from the most advanced ECMWF global reanalysis, ERA5. The added value of the regional CERRA data with respect to the global reanalysis products can be related to the higher horizontal resolution that permitted, in the modeling stage, the usage of a better description of the model topography and physiographic data, and the assimilation of more surface observations (CERRA, 2022). Indeed, CERRA dataset supplies weather reanalysis data specifically for the pan-European territory, for which the dataset is optimized, with a very high horizontal resolution (i.e., 5.5 km – Fig. 3). The vertical coverage spans from the surface to the top of the atmosphere: however, in the present study, only single levels were considered: at surface for solar radiation downwards and air pressure, at 10 m for wind speed and at 2 m for air temperature and relative humidity.

Reanalysis data in forecast mode are stored with hourly resolution for the CERRA dataset. The analysis products have, instead, 3-hourly temporal resolution. Analysis data at a certain hour are assumed to be of higher quality than the forecasts valid at the same hour, as they are on average closer to observations (CERRA, 2022). However, they are available only every three hours and not all parameters are available for the analyses. The forecast model starts from the analysis and the outputs are saved hourly for the first six hours.

In this study, analysis products were selected when available, such as for all weather variables except for solar radiation, for which the most recent available forecast at hourly resolution was selected instead. Then, the daily aggregations were performed by gathering the hourly for solar radiation or 3-hourly data available for each day of interest. Fig. 3 shows the numerical grid points of the CERRA model along with the AWS sites.

3. Methods

3.1. Downscaling and bias correction of reanalysis data

Weather reanalysis data are available at certain numerical grid points having a given horizontal spacing (Fig. 3). For the case of CERRA, the grid spacing is 5.5 km. For comparing the weather reanalysis outputs at these grid points with ground-based weather observations at the AWS sites, it is then needed to infer reanalysis data from the native grid points to the points where the AWSs are located. This procedure can be performed by applying statistical downscaling techniques.

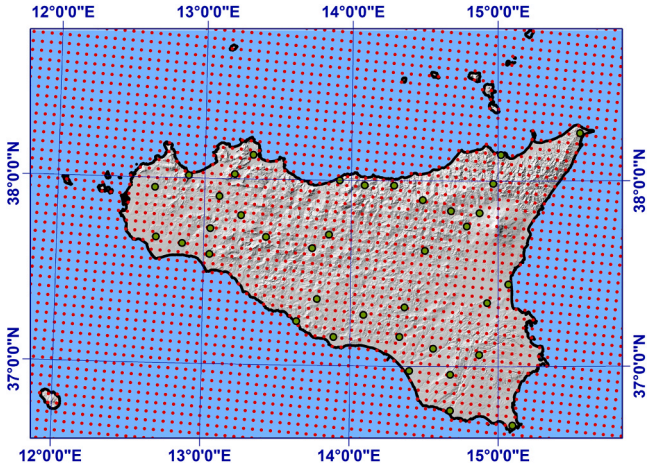

Fig. 3. Location of the CERRA grid points (red circles) with 5.5 km of horizontal spacing, compared with the sparse position of the AWS network (green circles).

Here, a triangle-based bi-linear interpolation method was employed (Lee and Schachter, 1980), by means of Delaunay triangulation. The method consists in considering the three grid points closest to the site where the estimate is needed and hypothesizing that the values of the variable of interest vary linearly between two points.

In accordance with a previous study in the region by Pelosi and Chirico (2021), we found statistical correlations between the daily maximum and minimum air temperatures and terrain elevation, so that before proceeding with the grid interpolation of these two weather variables, an environmental lapse rate (ELR) correction was applied to the grid points of interest for interpolation. This correction allows to consider the elevation differences between the numerical grid points and each AWS site by computing the rate of temperature change with elevation (i.e., ELR). The ELR for the region of interest was assessed thanks to all the observations of temperature available along the whole region at different sites with different elevations.

The environmental lapse rate depends on several and complex factors from the large-scale atmospheric circulation to local features related to topography or surface specific characteristics. The use of a linear lapse rate for elevation correction between model and station temperature is a common practice in hydrological and environmental applications (e.g., Gupta and Tarboton, 2016).

Here, we computed the ELR on monthly basis for the daily maximum and minimum air temperatures by employing all the available ground-based measurements of temperature in the region at 96 monitoring sites (www.sias.regione.sicilia.it), in the calibration period 2003–2008. The ELRs were assessed by means of linear regression models with elevation (Pelosi and Chirico, 2021). The assessment of ELRs from observations was preferred to the use of the common reference value of $-0.0065\ ^{\circ}C\ m^{-1}$ (Rolland, 2003; Gao et al., 2012), in accordance with literature recommendations for complex terrain and since we verified better performances in the estimates.

Table 3 shows the value of the estimated monthly ELR for T_{max} and T_{min} and the relative coefficients of determination, R^2_{ELR}. The rates vary from −0.0046 to −0.0064 for T_{max} and from −0.0027 to −0.0045 for T_{min}. Daily maximum air temperature shows on average a stronger linear correlation with elevation than minimum air temperature that tends to be more stable during the night as also found in other studies (e.g., Dutra et al., 2020).

For the other variables, no significant statistical correlations with elevation or other topographic features were found, so the downscaling was performed only with the chosen spatial interpolation technique with no further corrections.

However, in combination with the statistical downscaling, if a set of ground-based observations is available like in this study for a calibration period, it is preferable to proceed with statistical postprocessing techniques to partially remove the estimation errors made by the numerical models. These errors can be both systematic and non-systematic and they are mainly due to sub grid-scale variability and inability of the models to fully describe the physical phenomena occurring (Journée and Bertrand, 2010; Pelosi et al., 2017).

Statistical postprocessing can be performed in many ways from batch processing with a calibration dataset to sequential correction from a continuous series of observations. Then, in similar studies that used reanalysis data for assessing ET_O, it has been found that simple bias correction approaches are to be preferred to more sophisticated post-processing techniques, since no significant loss in accuracy is evident despite the much lower computation costs (e.g., Paredes et al., 2018).

In this study, a monthly constant value for bias correction of each weather variable was computed over the region in the calibration period that was set in years 2003–2008. However, it was verified that the six years of the calibration period may be chosen randomly among the available years of the time-series with no statistically meaningful changes in the bias correction. This circumstance is coherent with the hypothesis that each year of observation is independent and the

Table 3
Monthly environmental lapse rates (ELR) estimated for downscaling the daily T_{max} and T_{min}, the results are in accordance with Pelosi and Chirico (2021).

		APR	MAY	JUN	JUL	AUG	SEP
T_{max}	ELR	-0.0064	-0.0060	-0.0051	-0.0047	-0.0046	-0.0060
	R^2_{ELR}	0.82	0.64	0.43	0.36	0.40	0.73
T_{min}	ELR	-0.0035	-0.0033	-0.0027	-0.0029	-0.0033	-0.0045
	R^2_{ELR}	0.46	0.41	0.30	0.32	0.39	0.62

interannual variability of weather is random.

The applied method for bias correction consists in adding to the downscaled products the monthly regional mean difference (bias) between the ground-based measurements and the respective downscaled data, computed over the calibration period (Pelosi and Chirico, 2021). No bias correction was applied for wind speed, for which no systematic bias pattern was found, consistent with previous reports (Ricard and Anctil, 2019; Pelosi et al., 2020a; Pelosi and Chirico, 2021).

Then, the remaining 14 years (2009–2022) were used for creating the validation set to which the performance statistics refer. The choice of a batch bias correction approach was applied in the more cautelative and general scenario for which ground weather observations were not available for the period of interest, but data from a few past irrigation seasons (e.g., here six seasons over 20) were available for calibration. This scenario also justifies the use of reanalysis data as proxy of ground-based meteorological observations for all the motivations described in the Introduction.

3.2. Spatial interpolation of weather data

In this study, the performance evaluation of CERRA data is compared to the performance evaluation of the most widely used alternative way for assessing weather variable at ungauged locations when a monitoring network is available in a region, such as spatial interpolation. It is clear that if a ground-based weather observation is available, it represents the most accurate guess of a weather variable. However, this availability is limited to discrete monitoring sites. Moreover, the monitoring networks are generally sparse. Thus, assessing the values of weather variables at ungauged locations for regional studies, in the most opportune case with a working monitoring network, means spatially interpolating the available observations. Among spatial interpolation methods, geostatistical techniques are the most advanced and used for weather applications (Hofstra et al., 2008). Here, according to Pelosi and Chirico (2021), ordinary kriging was employed for spatial interpolation of wind speed, actual vapor pressure and solar radiation, while regression kriging with elevation was used for maximum and minimum air temperatures since statistical correlation exists between these weather variables and an auxiliary external variable, i.e., elevation, sampled with a higher spatial resolution (Prudhomme and Reed, 1999; Jarvis and Stuart, 2001; Furcolo et al., 2016).

The kriging interpolations give exact estimates at the sites where observations are available, so a common method to compute the kriging estimation errors consists of calculating the jackknife kriging estimates of the variable of interest at monitoring sites. These estimates were obtained by recursively applying the kriging interpolator to the observations available at the remaining sampling sites by excluding the site of interest for the error evaluation. This procedure is also known as leave-one-out cross-validation technique, and it allowed to evaluate the performance of the spatial interpolation of ground-based data.

Indeed, the result of the leave-one-out cross-validation technique was a set of interpolated ground-based data (IGD) at each AWS site that could be compared with the measurements recorded at the same site, for evaluating the performance of the kriging interpolator (Pelosi and Chirico, 2021).

In this study, the theoretical details of the kriging methods are omitted: for these, please refer to Journel and Huijbregts (1978) and Cressie (1993).

3.3. Assessment of daily reference evapotranspiration (ET_O)

In this study, according to previous studies on the topic, the daily reference evapotranspiration, ET_O (mm day^{-1}) was computed with the FAO Penman–Monteith equation (Allen et al., 1998), which is the most accurate formulation for the assessment of ET_O when a complete dataset of weather variables is available. The FAO Penman–Monteith equation refers to the rate of evapotranspiration from a hypothetical reference crop with an assumed crop height of 0.12 m, a fixed surface resistance of 70 s m^{-1} and an albedo of 0.23, closely resembling the evapotranspiration from an extensive surface of green grass of uniform height, actively growing, well-watered, free of water stress and disease and completely shading the ground. ET_O can be interpreted as a synthetic index of the influence of weather conditions on crops and it represents a key variable for assessing crop evapotranspiration and crop water requirements (e.g., Pelosi et al., 2022). According to the FAO Penman–Monteith equation, ET_O can be written as follows:

$$ET_O = \frac{1}{\lambda}\frac{\Delta(R_n - G) + \gamma\frac{900}{T+273}WS(e_s - e_a)}{\Delta + \gamma_p(1 + 0.34WS)} \quad (3)$$

where λ is the latent heat of vaporization, equal to 2.45 MJ kg^{-1}; Δ (kPa $°C^{-1}$) is the slope of the vapor pressure curve; γ is the psychometric constant (kPa $°C^{-1}$); T (°C) is the daily mean air temperature measured at 2 m height and computed as the average between the daily maximum (T_{max}) and minimum (T_{min}) air temperature measured at 2 m height; WS (m s^{-1}) is the wind speed at 2 m height above ground; e_s (kPa) and e_a (kPa) are, respectively, the daily saturation vapor pressure and daily actual vapor pressure (Eqs. 1–2) needed for the computation of the saturation vapor pressure deficit (e_s - e_a); R_n (MJ m^{-2} day^{-1}) is the net radiation at the crop surface, calculated as the difference between the incoming net shortwave radiation and the outgoing net long-wave radiation. The incoming net shortwave radiation is a fraction of the incoming shortwave solar radiation (R_S), computed for the reference crop by setting the albedo equal to 0.23 (i.e., albedo of the reference crop).

Finally, G (MJ m^{-2} day^{-1}) is the soil heat flux density that was computed, as suggested by Allen et al. (1998), with the formula proposed by Choudhury et al. (1987) and considering the leaf area index of the reference crop equal to 2.88, as follows:

$$G = 0.4R_n\exp[-0.5LAI] \quad (4)$$

In this study, since the observed wind speed at the ground based AWSs was measured at 10 m height ($WS_{10\,m}$), the wind speed at 2 m, WS (m s^{-1}), was obtained by using a logarithmic wind speed profile as suggested by Allen et al. (1998) that led to a reduction factor of about 0.748.

3.4. Statistical indices for estimation performance

The performance indicators were selected among those commonly used for analogous previous studies (e.g., Paredes et al., 2021; Pelosi and Chirico, 2021):

(i) The percent BIAS (PBIAS, %), which is used as an indicator of accuracy:

$$\text{PBIAS}\ (\%) = \frac{1}{\overline{O}} \frac{\sum_{i=1}^{n}(P_i - O_i)}{n} 100 \quad (5)$$

where P_i and O_i are, respectively, the variable for which the performance evaluation is desired, i.e., IGD and CERRA data, and the corresponding observed variable (assumed, here, as benchmark) at the i^{th} day; n denotes the number of examined days and $\overline{O}$ is the mean of the observations computed over the examined days. The more the PBIAS differs from zero, the less accurate is the estimate. PBIAS < 0 suggests on average underestimation while PBIAS > 0 overestimation.

(ii) The percent normalized root mean square error (NRMSE, %) which gives insight into both accuracy and precision:

$$\text{NRMSE}(\%) = \frac{1}{\overline{O}} \sqrt{\frac{\sum_{i=1}^{n}(P_i - O_i)^2}{n}} 100 \quad (6)$$

The greater is the NRMSE, the less accurate and precise are the estimates.

(iii) The coefficient of determination (R^2) of the ordinary least squares regression model is used to assess the dispersion of pairs of O_i and P_i (independent variable) values along the regression line:

$$R^2 = \frac{\sum_{i=1}^{n}(\widehat{O}_i - \overline{O})^2}{\sum_{i=1}^{n}(O_i - \overline{O})^2} \quad (7)$$

where $\widehat{O}_i$ is the predicted value by the linear regression $\widehat{O}_i = a + bP_i$. R^2 may vary from 0 to 1: the closer R^2 values are to 1, the larger the fraction of the variance of the observations explained by the linear model.

(iv) The Nash and Sutcliffe (1970) model efficiency (NSE) is equal to one minus the sum of the absolute squared differences between the predicted and observed values normalized by the variance of the observed values during the period of interest (Krause et al., 2005):

$$\text{NSE} = 1 - \frac{\sum_{i=1}^{n}(P_i - O_i)^2}{\sum_{i=1}^{n}(O_i - \overline{O})^2} \quad (8)$$

The range of NSE lies between 1 (perfect model with an estimation error variance equal to zero) and $-\infty$. Values of NSE nearer to 1 suggest a model with more predictive skill. NSE equal to 0 indicates that the model has the same predictive skill as the mean of the data, in terms of the sum of the squared error. An NSE value lower than zero indicates that the mean value of the observed data would have been a better predictor than the model that shows an estimation error variance which is significantly larger than the variance of the observations (Pelosi and Chirico, 2021).

4. Results and discussion

4.1. Performance of CERRA reanalysis weather variables

In this section, the results about performance of CERRA reanalysis weather variable outputs are shown by using the statistical indices described above and, as benchmarks for the weather truth, the ground-based observations of the same variables at the 38 AWSs, available in the region. The found statistical index values at 38 AWS sites are then provided with boxplots that give insight about their distribution along the region: in particular, on each boxplot, the mean values of the indices are displayed with a black solid circle mark while the median values are specified with horizontal marks in the box, whose edges are the 25th, q_1, and 75th, q_3, percentiles of data. Then, each boxplot shows whiskers that extend to the most extreme data values not considered outliers, and outliers are plotted individually. The points are drawn as outliers if they are larger than $q_3 + 1.5(q_3–q_1)$ or smaller than $q_1 - 1.5(q_3–q_1)$. Beside CERRA performances, IGD performances are reported. The IGD data were obtained at each AWS by the leave-one-out cross-validation technique and then, compared to the ground-based observations for the computation of the statistical indices. The CERRA data were downscaled from the native grid points to the AWS sites and the bias correction was applied by considering the bias in the calibration period, as described in the previous sections.

The data object of the current performance evaluation refers to the validation period (i.e., 2009–2022 – validation set).

The weather variables, for which results are here provided are daily maximum and minimum air temperature at 2 m (Figs. 4–5), daily mean wind speed at 10 m (Fig. 6), daily mean actual vapor pressure (Fig. 7) and daily mean incoming shortwave solar radiation (Fig. 8).

Fig. 4 refers to the performance of IGD and CERRA daily maximum air temperature. The mean PBIAS for CERRA in the region is 1.2%, showing a negligible overestimation of the variable. For CERRA data, the mean NRMSE is 5.8%, with two outliers exhibiting a NRMSE of 12% and 11% at AWS n. 14 and n. 36, both located in the mountainous area in the north-eastern part of the island. The values of R^2 are always above 0.90: this circumstance means a very satisfactory linear correlation between CERRA data and observations in the region, for what concern T_{max}. The NSE is above 0.80 for CERRA and 0.40 for IGD, showing excellent predictive performances for CERRA T_{max} than IGD. Also, the other IGD performance indexes are slightly worse than CERRA ones: the mean PBIAS and NRMSE are equal to 1.8% and 5.9%, respectively; then, the outliers of the NRMSE for IGD T_{max} are 12% and 17%. R^2 assumes very high values, above 0.88 and, with a wider range of variation over the region than the R^2 of CERRA T_{max}.

T_{max} is the weather variable that shows the best performances in terms of accuracy and reliability: this outcome is coherent with the findings of other studies concerning ERA5 and ERA5-Land (Pelosi et al., 2020a; Pelosi and Chirico, 2021; Vanella et al., 2022) as well as other reanalysis products, such as NCEP/NCAR-PrincUV (e.g., Raziei and Parehkar, 2021). Moreover, for the same region, CERRA slightly outperforms ERA5-Land for T_{max} estimates (Pelosi and Chirico, 2021).

Fig. 5 shows the performance of IGD and CERRA daily minimum air temperature: those are both worse than the ones obtained for daily maximum air temperature. As also pointed out in other studies on reanalysis products (e.g., Pelosi and Chirico, 2021; Vanella et al., 2022), the main reason lies in the major spatial variability of T_{min} with respect to T_{max} over a region, associated to a strong dependence on local topographic conditions, besides elevation, which represent a sub-grid information for CERRA and unexplained variance sources for kriging. The PBIAS and NRMSE are, on average, equal to 0.93% and 13%, respectively, for CERRA, and equal to −0.35% and 11%, for IGD. For CERRA data, the 25th and 75th percentile are equal to −6.4% and 8.4% for the PBIAS while 9.1% and 17% for the NRMSE that shows an outlier of 32% at AWS n. 2 in the hilly inner part of the island. The values of R^2 are above 0.84 for CERRA and 0.89 for IGD. The NSE values are always positive and above 0.62 for IGD and 0.40 for CERRA. Overall, for T_{min}, the spatial interpolation works slightly better than CERRA. The performance of CERRA and ERA5-Land (Pelosi and Chirico, 2021) for T_{min} are similar: however, for the same study area, ERA5-Land shows an outlier on the coast due to the limitations associated with its domain that extends only over land.

The IGD and CERRA daily mean wind speed estimates show the worst performance among all the variables analyzed (Fig. 6). For CERRA data, this evidence, among other factors, is also due to the lack of the bias correction since no systematic bias pattern was found for this weather variable, in agreement with previous similar reports relative to southern Italy and ECMWF products (Pelosi et al., 2020a; Pelosi and Chirico, 2021). However, this finding can be also found in other studies outside Italy, in countries with different climate and topography as well

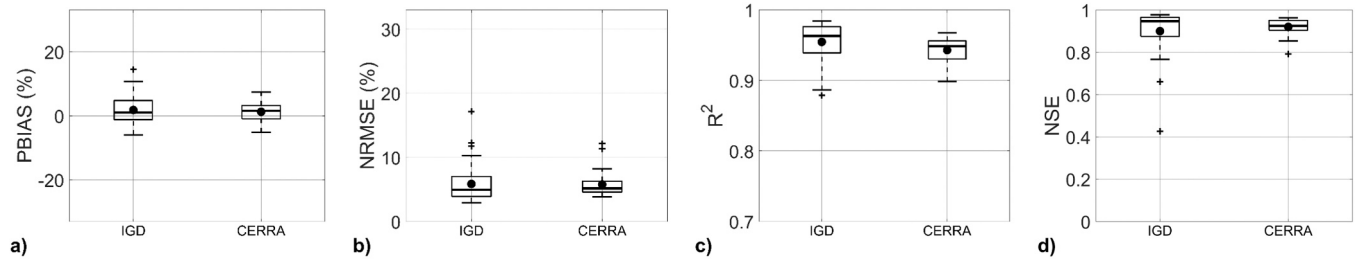

Fig. 4. Statistical indices of daily T_{max} at 38 AWS sites (validation set).

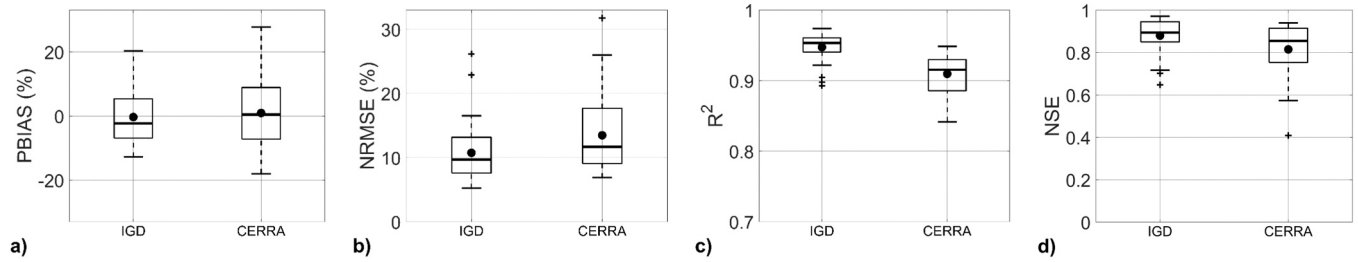

Fig. 5. Statistical indices of daily T_{min} at 38 AWS sites (validation set).

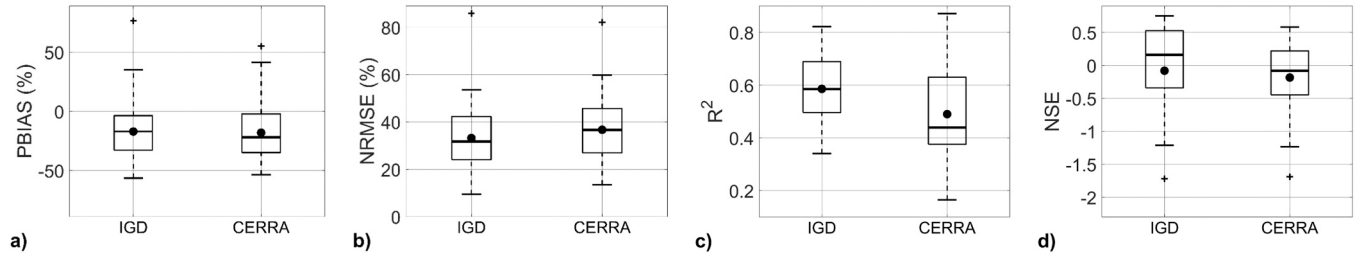

Fig. 6. Statistical indices of daily $WS_{10\,m}$ at 38 AWS sites (validation set).

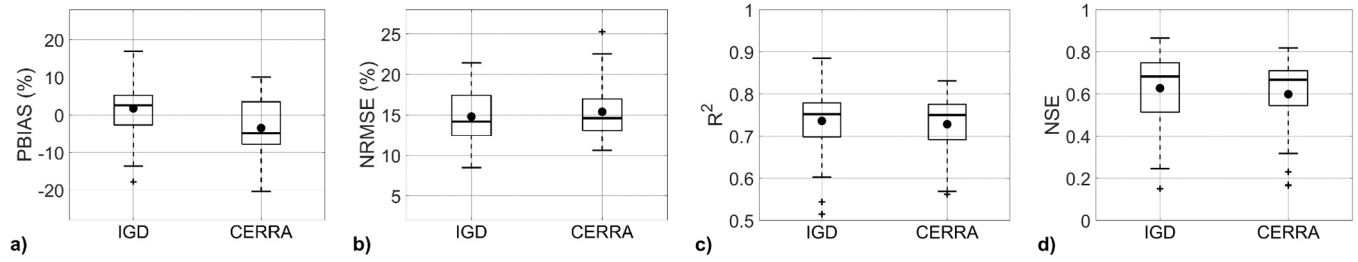

Fig. 7. Statistical indices of daily e_a at 38 AWS sites (validation set).

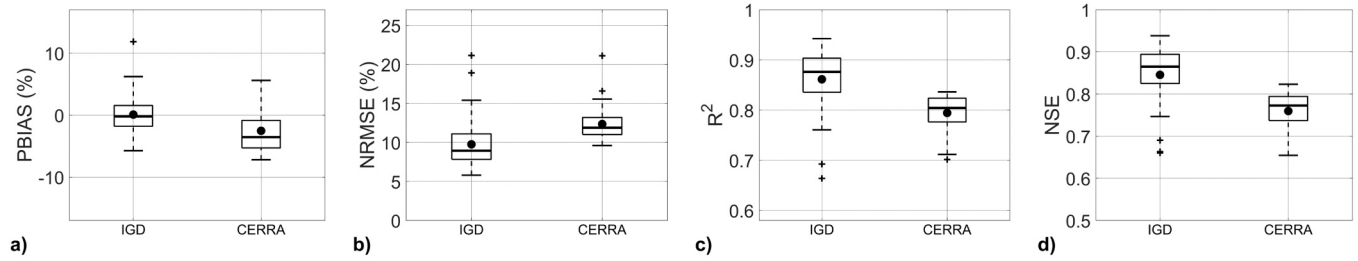

Fig. 8. Statistical indices of daily R_S at 38 AWS sites (validation set).

as for NCEP/NCAR-PrincUV model (e.g., Raziei and Parehkar, 2021). The main reason relies in the fact that wind speed is not a prognostic variable, therefore it is affected by greater prediction errors due to the major uncertainties of the model formulation of the ongoing atmospheric processes (Pelosi et al., 2017). For the IGD case, the reason may be found in the complex spatial variability of the data that show a sub-grid scale variability that cannot be accurately interpreted by spatial interpolation. The mean PBIAS and NRMSE are equal to −18% and 37%, respectively, for CERRA and −17% and 33%, respectively, for IGD. For both databases, the NRMSE has a peak above 80% at AWS n. 17 located in a windy area on the coast with hills in the background. The values of R^2 are very irregular, ranging from 0.16 to 0.89 for both estimates. The NSE index shows negative values for about half of the stations: this finding means that the observed mean could be considered a better predictor than the IGD and CERRA estimates. The low accuracy and reliability of wind speed estimates are a common finding among reanalysis databases and, in windy areas, can represent a severe issue, especially due to the high sensitivity of evapotranspiration on wind speed performances (Nouri et al., 2022).

About the performances of the daily mean actual vapor pressure (Fig. 7), the mean PBIAS and mean NRMSE are, respectively, −3.5% and 15% for CERRA and 1.7% and 14% for IGD. The NRMSE shows an outlier equal to 25% for CERRA estimates. The values of R^2 are above 0.56. The values of the NSE are always positive, although above 0.20, with mean around 0.60 for both databases. The performances for IGD are slightly better than those showed by CERRA e_a, and in perfect accordance with the results found for ERA5-Land for the same region and, in general, for Southern Italy (Pelosi et al., 2020a; Pelosi and Chirico, 2021). Similarly, Raziei and Parehkar (2021) found that large estimation errors are associated with air relative humidity, from which the actual vapor pressure is derived.

Lastly, as reported in Fig. 8, the CERRA incoming solar radiation has a mean PBIAS equal to −2.5% while IGD R_S shows a mean PBIAS almost equal to zero. The mean NRMSE is 12% and 10% for CERRA and IGD, respectively; the major outliers for the NRMSE reach the value of about 21% for both databases. The values of R^2 range from 0.66 to 0.94: better linear correlation between estimates and observations are, on average, found for IGD. The values of NSE are on average better for IGD than CERRA but both databases provide NSE values above 0.65.

CERRA R_S shows very similar performances than ERA5-Land R_s provided for the same region by Pelosi and Chirico (2021) that already demonstrated better performances of ERA5-Land R_S than ERA5 and the former ERA-Interim. They also proposed, as alternative to NWP outputs for R_S estimates, satellite-based CM-SAF solar radiation data in accordance with Paredes et al. (2021) that, for the first time in literature, proposed satellite-based solar radiation products for assessing reference evapotranspiration as alternative to the use of ERA5 solar radiation estimates.

Overall, CERRA performances related to the analyzed weather variables are similar to ERA5-Land performances for the same region, described in Pelosi and Chirico (2021), despite the finer spatial resolution of the CERRA numerical grid that did not contribute to a significant improvement of the accuracy and reliability of the reanalysis outputs. However, if compared with the former ECMWF regional reanalysis database, UERRA MESCAN-SURFEX, analyzed by Pelosi et al. (2020a), CERRA show better performance indices and more accurate and reliable outputs that reflect the improvements in forecast skill from ERA-Interim to ERA5.

4.2. Efficiency of the bias correction technique

Here, some brief results about the efficiency of the bias correction technique applied to CERRA weather variables are presented. Overall, the bias correction improved mean PBIAS and mean NRMSE as specified in Table 4. On the contrary, the value of R^2 remained constant or slightly worsened. For wind speed, no bias correction was applied.

Table 4
Mean performance of CERRA weather variables before and after bias correction (BC).

	Mean PBIAS (%)	Mean NRMSE (%)	Mean R^2
T_{max} before BC	-4.8	8.1	0.94
T_{max} after BC	1.2	5.8	0.94
T_{min} before BC	10.2	15.8	0.91
T_{min} after BC	0.93	13.5	0.91
e_a before BC	16.	21.3	0.76
e_a after BC	-3.5	15.4	0.73
R_S before BC	3.2	12.5	0.79
R_S after BC	-2.5	12.3	0.79

For both T_{max} and T_{min}, after bias correction, the mean NRMSE decreased by about 2% while the mean PBIAS decreased by about 4% and 9%, respectively. The R^2 remained unchanged. For the actual vapor pressure, after bias correction, the mean PBIAS and mean NRMSE decreased by about 13% and 6%, respectively. Solar radiation showed very good performance before bias correction so after bias correction the improvements were negligible.

4.3. Computation of reference evapotranspiration by using ground-based weather data

Some statistics related to the reference evapotranspiration computed with Eq. 3 by using the observed ground weather data are here reported to arrange the following discussion about the performance of the ET_O estimates by using the CERRA data as alternative.

Table 5 reports monthly statistics of the daily ET_O averaged between the 38 AWSs over the irrigation seasons of the years 2003–2020.

The minimum monthly mean of daily ET_O was recorded in April (3.28 mm day^{-1}) and the maximum in July (5.74 mm day^{-1}) as expected in consideration of the Mediterranean climate of the region. The mean coefficient of variation was lowest in July (0.14) and highest in April (0.31) that indicates that more stable conditions are found in summer than in spring. These statistics refer to average values over the region that, as already said, is characterized by greater spatial variability of weather due to a complex and varied topography. The pattern of the monthly average of daily ET_O (Fig. 9) mainly follows the spatial variability of the air temperature over the island (Fig. 2a), showing greater values on the coasts, especially in the south-western part of the region.

4.4. Performance of daily reference evapotranspiration estimates by using CERRA data

This section contains the main results of the study related to the use of CERRA agrometeorological data as inputs of the FAO Penman–Monteith equation for daily ET_O assessment, compared with the alternative use of ground-based observations. Moreover, the same evaluations are given with respect to the use of spatial interpolated data as input data when observations in a certain site are unavailable, but a monitoring network is working. For the scope, Fig. 10 shows the statistical indices PBIAS, NRMSE, R^2 and NSE.

The mean PBIAS are −2.7% and 5.6% for CERRA and IGD, respectively, while the mean NRMSE values for both are equal to 13%. The

Table 5
Monthly statistics of the daily reference evapotranspiration over the region, based on data recorded during 20 irrigation seasons (2003–2022).

ET_O (mm day^{-1})	Mean	Coefficient of variation
April	3.28	0.31
May	4.26	0.26
June	5.23	0.21
July	5.74	0.14
August	5.12	0.18
September	3.55	0.25

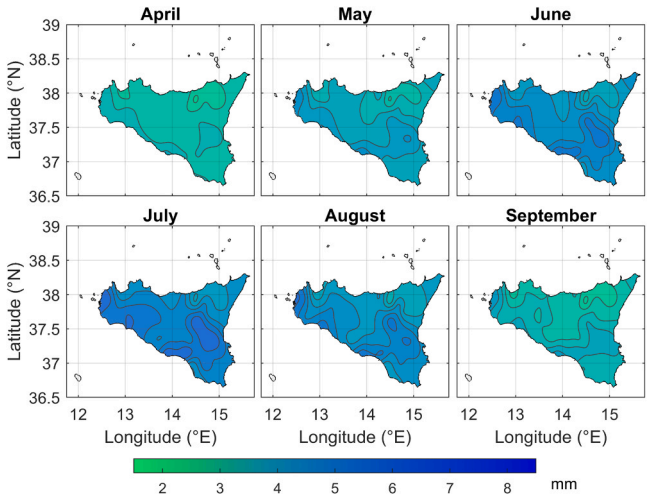

Fig. 9. Spatial variation over the region of the monthly average daily reference evapotranspiration.

NRMSE shows an outlier value equal to 28% and 24% for IGD and CERRA, respectively. These values are found at the AWS n. 17, where the wind speed shows the worst performance. The outcome agrees with the findings about the sensitivity of ET_O estimates to errors in input weather variables, made by Pelosi and Chirico (2021). Indeed, in that study, it was found that the largest errors in ET_O estimates are obtained when WS ground data are replaced with reanalysis wind data.

The values of R^2 range from 0.64 to 0.93: IGD shows on average a R^2 equal to 0.85, rather than CERRA that presents a mean R^2 equal to 0.82; however, IGD shows slightly smaller extreme values. NSE values are always greater than zero for CERRA ET_O estimates with a mean value of about 0.70, while IGD shows a negative NSE value at AWS n.17, and overall, a mean NSE equal to 0.66.

The ET_O estimates with both IGD and CERRA data have very similar performance and overall high quality. The improvements of the ET_O performances by using CERRA rather than ERA5-Land are negligible since, for ERA5-Land ET_O estimates, the mean PBIAS and NRMSE were 2.8% and 14%, respectively; while the mean R^2 and NSE were 0.76 and 0.67, respectively (Pelosi and Chirico, 2021).

Lastly, Fig. 11 shows the spatial variability of the errors, in terms of PBIAS and NRMSE, made by three different sources of weather data for the ET_O assessment. ET_O estimates tend to be less accurate in mountainous areas and on the coast, especially in the south-western side of the

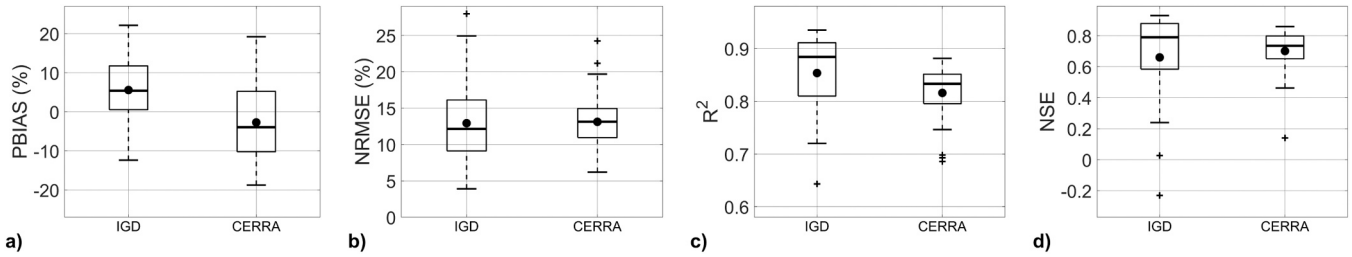

Fig. 10. Statistical indices of daily ET_O at 38 AWS sites (validation set).

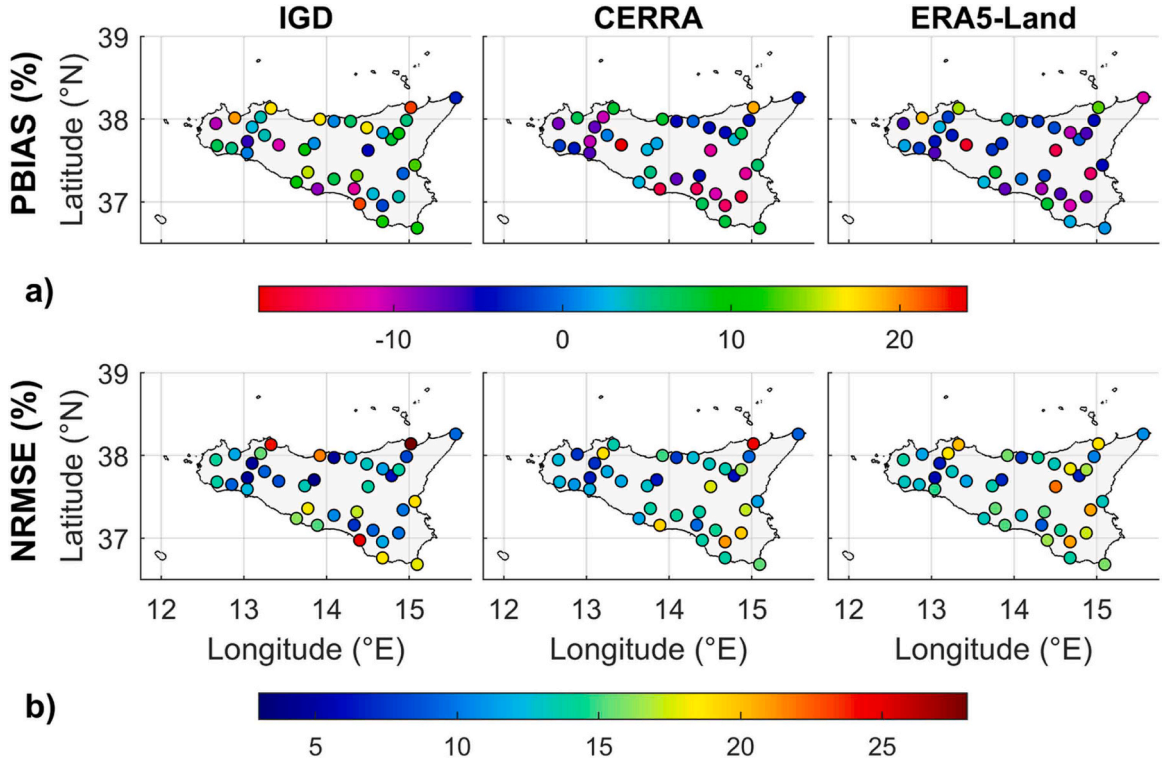

Fig. 11. Map showing the variations, in terms of a) PBIAS and, b) NRMSE, of daily ET_O with respect to observations, for the IGD, CERRA and ERA5-Land estimates.

island. Moreover, the sites with larger errors in wind speed estimates are also subject to major errors in ET_O estimates. One limitation of ERA5-Land data relies in the availability of data only over land, causing possible uncertainties along the coasts. However, both CERRA and ERA5-Land show similar error patterns along the region, slightly different from the IGD case since they are both products of the same numerical model despite the different parametrization, numerical grid, and optimization algorithms.

5. Conclusions

Reanalysis products represent important weather data sources for the regional assessment of the hydrological variables relevant to water resource management and climate studies. Several studies implemented different reanalysis databases to assess reference evapotranspiration at regional scale (among others, Martins et al., 2017; Pelosi and Chirico, 2021; Raziei and Parehkar, 2021). However, reanalysis products are constantly updated following the scientific and technological developments that lead to NWP models with increasing weather forecast skills. The latest ECMWF regional reanalysis database is CERRA, released in August 2022.

In this study, for the first time, the performances of CERRA data were compared with the spatial interpolated values of the ground observations (IGD) at 38 AWSs in Sicily, during the irrigation seasons of years 2009–2022. By assuming that each year of observation is independent and the interannual variability of weather is random, years 2003–2008 were used as calibration period for bias-correcting CERRA data, under the hypothesis that users have observations for only few irrigation seasons and reanalysis data were then used as unique available source of data in the validation period. This hypothesis made the findings of the study more general, however further improvements in CERRA performances may be obtained if weather observations were available for the whole period of analysis and then, usable for bias correcting the reanalysis products by computing the bias in the whole period itself rather than for a few years in the calibration period. In this case, the comparison between the two data sources would be fairer, since the IGD can be applied only if a monitoring network is working, and, except for the monitored sites for which the ground measure is the truth, CERRA estimates would be preferred at unmonitored sites, where IGD would be even slightly outperformed.

Indeed, in spite of the said conservative hypothesis for CERRA data, the outcomes showed that CERRA performances are similar to the IGD performances for all the examined weather variables, such as air temperature (which is the most accurate), actual vapor pressure, solar radiation, and wind speed. Both CERRA and IGD performances are excellent, except for wind speed that shows the least accuracy, especially in hilly areas with complex terrain. However, when used as inputs for assessing reference evapotranspiration, both CERRA and IGD sets of weather data provided precise and accurate ET_O estimates that show mean PBIAS values slightly below 6% and mean NRMSE values of about 13% in the region.

Other studies already demonstrated that among the available ECMWF reanalysis data, ERA5-Land outputs were the most accurate for the assessment of ET_O both in comparison withERA5 (Vanella et al., 2022) and the outdated regional reanalysis, such as UERRA MESCAN-SURFEX forced by the former global ERA-Interim reanalysis (Pelosi et al., 2020a). Here, we demonstrated that the regional reanalysis CERRA available over Europe at a spatial resolution of 5.5 km slightly outperformed ERA5-Land that has instead a resolution of 9 km and covers just the land component of the globe, resulting in major biases and uncertainties close to the coasts (Pelosi and Chirico, 2021).

Among other applications, the availability of reliable gridded estimates of ET_O at regional scale represents a major contribution for the quantitative assessment of irrigation volumes since, besides crop and soil properties, ET_O is a key variable in crop-water-balance models, and it summarizes the influence of weather conditions on crop water requirements. Therefore, the knowledge of its past and average patterns in space and time over a region and during a season can be fundamental in water management studies for the allocation of the resources among competitive uses and territories as well as for the exploitation of structural and investments funds within the EU Common Agricultural Policy, in compliance with the Water Framework Directive (2000/60/EC) and Regulation (EU) No 1303/2013 for the long-term sustainability of irrigated agriculture in open field.

In conclusion, the study contributed to the informed use of the newest CERRA reanalysis database for water management applications in a region with a Mediterranean climate. The results confirmed that regional reanalysis data represent a valid proxy of ground-based agrometeorological data for assessing ET_O in agricultural water management studies, especially in data-sparse regions for which the spatial interpolation of ground weather data is prone to large uncertainties, or when ground weather data cannot be easily gathered due to the inaccessibility and lack of interoperability of ground-based weather databases.

Declaration of Competing Interest

The authors declare that they have no known competing financial interests or personal relationships that could have appeared to influence the work reported in this paper.

Data availability

Data will be made available on request.

Acknowledgements

The paper contains modified Copernicus Climate Change Service information (Schimanke et al., 2021): the CERRA reanalysis data are Copernicus products belonging to European Union and accessible on the ECMWF Copernicus Climate Data Store (CDS - https://cds.climate.copernicus.eu). Ground weather data were provided by SIAS regional service (http://www.sias.regione.sicilia.it).

References

Albano, C.M., Abatzoglou, J.T., McEvoy, D.J., Huntington, J.L., Morton, C.G., Dettinger, M.D., Ott, T.J., 2022. A multidataset assessment of climatic drivers and uncertainties of recent trends in evaporative demand across the continental United States. J. Hydrometeor. 23, 505–519. https://doi.org/10.1175/JHM-D-21-0163.1.

Allen, R.G., 1996. Assessing integrity of weather data for use in reference evapotranspiration estimation. J. Irrig. Drain. Eng. 122 (2), 97–106. https://doi.org/10.1061/(ASCE)0733-9437(1996)122:2(97).

Allen, R.G., 2000. Using the FAO-56 dual crop coefficient method over an irrigated region as part of an evapotranspiration intercomparison study. J. Hydrol. 229, 27–41. https://doi.org/10.1016/S0022-1694(99)00194-8.

Allen, R.G., Pereira, L.S., Raes, D., Smith, M., 1998. Crop Evapotranspiration. Guidelines for Computing Crop Water Requirements. Paper 56 FAO Irrigation and Drainage. FAO,, Rome, p. 300. Paper 56.

Bauer, P., Thorpe, A., Brunet, G., 2015. The quiet revolution of numerical weather prediction. Nature 525, 47–55. https://doi.org/10.1038/nature14956.

Berndt, C., Haberlandt, U., 2018. Spatial interpolation of climate variables in Northern Germany—Influence of temporal resolution and network density. J. Hydrol. Reg. Stud. 15, 184–202. https://doi.org/10.1016/j.ejrh.2018.02.002.

Boulard, D., Castel, T., Camberlin, P., Sergent, A.-S., Bŕeda, N., Badeau, V., Rossi, A., Pohl, B., 2016. Capability of a regional climate model to simulate climate variables requested for water balance computation: a case study over northeastern France. Clim. Dyn. 46, 2689–2716.

Calera, A., Campos, I., Osann, A., D'Urso, G., Menenti, M., 2017. Remote sensing for crop water management: from ET modelling to services for the end users. Sensors 17, 1104. https://doi.org/10.3390/s17051104.

CERRA, User Guide. Copernicus European Regional ReAnalysis (CERRA): product user guide. Available at ⟨https://confluence.ecmwf.int/display/CKB/Copernicus+European+Regional+ReAnalysis+%28CERRA%29%3A+product+user+guide⟩ (Accessed on 29 August 2022).

Chirico, G.B., Pelosi, A., De Michele, C., Falanga Bolognesi, S., D'Urso, G., 2018. Forecasting potential evapotranspiration by combining numerical weather predictions and visible and near-infrared satellite images: an application in southern Italy. J. Agric. Sci. 156, 702–710. https://doi.org/10.1017/S0021859618000084.

Choudhury, B.J., Idso, S.B., Reginato, R.J., 1987. Analysis of an empirical model for soil heat flux under a growing wheat crop for estimating evaporation by an infrared temperature based energy balance equation. Agric. Meteorol. 39, 283–297.
Cressie, N., 1993. Statistics for Spatial Data. John Wiley and Sons,, New York, NY, USA.
Dutra, E., Muñoz Sabater, J., Boussetta, S., Komori, T., Hirahara, S., Balsamo, G., 2020. Environmental lapse rate for high-resolution land surface downscaling: an application to ERA5. Earth Space Sci. 7, e2019EA000984 https://doi.org/10.1029/2019EA000984.
Furcolo, P., Pelosi, A., Rossi, F., 2016. Statistical identification of orographic effects in the regional analysis of extreme rainfall. Hydrol. Process. 30, 1342–1353. https://doi.org/10.1002/hyp.10719.
Gao, L., Bernhardt, M., Schulz, K., 2012. Elevation correction of ERA-Interim temperature data in complex terrain. Hydrol. Earth Syst. Sci. 16, 4661–4673. https://doi.org/10.5194/hess-16-4661-2012.
Gupta, A.S., Tarboton, D.G., 2016. A tool for downscaling weather data from large-grid reanalysis products to finer spatial scales for distributed hydrological applications. Environ. Model. Softw. 84, 50–69. https://doi.org/10.1016/j.envsoft.2016.06.014.
Hersbach, H., Bell, B., Berrisford, P., et al., 2020. The ERA5 global reanalysis. Q J. R. Meteor. Soc. 146, 1999–2049. https://doi.org/10.1002/qj.3803.
Hofstra, N., Haylock, M., New, M., Jones, P., Frei, C., 2008. Comparison of six methods for the interpolation of daily, European climate data. J. Geophys. Res. Atmos. 113, D21110 https://doi.org/10.1029/2008JD010100.
Iglesias, A., Garrote, L., 2015. Adaptation strategies for agricultural water management under climate change in Europe. Agric. Water Manag. 155, 113–124. https://doi.org/10.1016/j.agwat.2015.03.014.
Irvem, A., Ozbuldu, M., 2022. Evaluation of the performance of CFSR reanalysis data set for estimating reference evapotranspiration (ET_O) in Turkey. Italian J. Agrometeorol. 2, 49–61. https://doi.org/10.36253/ijam1325.
Jarvis, C.H., Stuart, N., 2001. A comparison among strategies of interpolating maximum and minimum daily air temperatures. Part I: the selection of "guiding" topographic and land cover variables. J. Appl. Meteor. 40, 1060–1074. https://doi.org/10.1175/1520-0450(2001)040<1075:ACASFI>2.0.CO;2.
Journée, M., Bertrand, C., 2010. Improving the spatio-temporal distribution of surface radiation data by merging ground and satellite measurements. Remote Sens. Environ. 114 (11), 2692–2704. https://doi.org/10.1016/j.rse.2010.06.010.
Journel, A.G., Huijbregts, C.J., 1978. Mining Geostatistics. Academic Press,, London, UK.
Lee, D.T., Schachter, B.J., 1980. Two algorithms for constructing a Delaunay triangulation. Intern. Comput. Inform. Sci. 9, 219–242.
Liuzzo, L., Bono, E., Sammartano, V., Freni, G., 2017. Long-term temperature changes in Sicily, Southern Italy. Atmos. Res. 198, 44–55. https://doi.org/10.1016/j.atmosres.2017.08.007.
Longo-Minnolo, G., Vanella, D., Consoli, S., Intrigliolo, D.S., Ramírez-Cuestac, J.M., 2020. Integrating forecast meteorological data into the ArcDualKc model for estimating spatially distributed evapotranspiration rates of a citrus orchard. Agric. Water Manag. 231, 105967 https://doi.org/10.1016/j.agwat.2019.105967.
Martins, D.S., Paredes, P., Raziei, T., Pires, C., Cadima, J., Pereira, L.S., 2017. Assessing reference evapotranspiration estimation from reanalysis weather products. An application to the Iberian Peninsula. Int. J. Climatol. 37, 2378–2397. https://doi.org/10.1002/joc.4852.
Medina, H., Tian, D., Srivastava, P., Pelosi, A., Chirico, G.B., 2018. Medium-range reference evapotranspiration forecasts for the contiguous United States based on multi-model numerical weather predictions. J. Hydrol. 562, 502–517. https://doi.org/10.1016/j.jhydrol.2018.05.029.
Merino, R.A., Gassmann, M.I., 2023. Trends of reference evapotranspiration and its physical drivers in southern South America. Int. J. Climatol. 43 (3), 1593–1609. https://doi.org/10.1002/joc.7935.
Nouri, M., Homaee, M., 2022. Reference crop evapotranspiration for data-sparse regions using reanalysis products. Agric. Water Manag. 262, 107319 https://doi.org/10.1016/j.agwat.2021.107319.
Nouri, M., Ebrahimipak, N.A., Hosseini, S.N., 2022. Estimating reference evapotranspiration for water-limited windy areas under data scarcity. Theor. Appl. Clim. 150, 593–611. https://doi.org/10.1007/s00704-022-04182-6.
Paredes, P., Martins, D.S., Pereira, L.S., Cadima, J., Pires, C., 2018. Accuracy of daily estimation of grass reference evapotranspiration using ERA-Interim reanalysis products with assessment of alternative bias correction schemes. Agric. Water Manag. 210, 340–353. https://doi.org/10.1016/j.agwat.2018.08.003.
Paredes, P., Trigo, I., de Bruin, H., Simões, N., Pereira, L.S., 2021. Daily grass reference evapotranspiration with Meteosat Second Generation shortwave radiation and reference ET products. Agric. Water Manag. 248, 106543 https://doi.org/10.1016/j.agwat.2020.106543.
Peel, M.C., Finlayson, B.L., McMahon, T.A., 2007. Updated world map of the Köppen–Geiger climate classification. Hydrol. Earth Syst. Sci. 11, 1633–1644. https://doi.org/10.5194/hess-11-1633-2007.
Pelosi, A., Chirico, G.B., 2021. Regional assessment of daily reference evapotranspiration: can ground observations be replaced by blending ERA5-Land meteorological reanalysis and CM-SAF satellite-based radiation data. Agric. Water Manag. 258, 107169 https://doi.org/10.1016/j.agwat.2021.107169.
Pelosi, A., Medina, H., Villani, P., D'Urso, G., Chirico, G.B., 2016. Probabilistic forecasting of reference evapotranspiration with a limited area ensemble prediction system. Agric. Water Manag. 178, 106–118. https://doi.org/10.1016/j.agwat.2016.09.015.
Pelosi, A., Medina, H., Van den Bergh, J., Vannitsem, S., Chirico, G.B., 2017. Adaptive Kalman filtering for post-processing of ensemble numerical weather predictions. Mon. Weather Rev. 145, 4837–4854. https://doi.org/10.1175/MWR-D-17-0084.1.
Pelosi, A., Terribile, F., D'Urso, G., Battista Chirico, G., 2020a. Comparison of ERA5-Land and UERRA MESCAN-SURFEX reanalysis data with spatially interpolated weather observations for the regional assessment of reference evapotranspiration. Water 12, 1669. https://doi.org/10.3390/w12061669.
Pelosi, A., Villani, P., Falanga Bolognesi, S., Chirico, G.B., D'Urso, G., 2020b. Predicting crop evapotranspiration by integrating ground and remote sensors with air temperature forecasts. Sensors 20, 1740. https://doi.org/10.3390/s20061740.
Pelosi, A., Belfiore, O.R., D'Urso, G., Chirico, G.B., 2022. Assessing crop water requirement and yield by combining ERA5-Land reanalysis data with CM-SAF satellite-based radiation data and Sentinel-2 satellite imagery. Remote Sens. 14, 6233. https://doi.org/10.3390/rs14246233.
Pereira, L.S., 2017. Water agriculture and food: challenges and issues. Water Resour. Manag. 31, 2985–2999. https://doi.org/10.1007/s11269-017-1664-z.
Perera, K.C., Western, A.W., Nawarathna, B., George, B., 2014. Forecasting daily reference evapotranspiration for Australia using numerical weather prediction outputs. Agric. Meteorol. 125, 305–313. https://doi.org/10.1016/j.agrformet.2014.03.014.
Pey, J., Querol, X., Alastuey, A., Forastiere, F., Stafoggia, M., 2013. African dust outbreaks over the Mediterranean Basin during 2001–2011: PM10 concentrations, phenomenology and trends, and its relation with synoptic and mesoscale meteorology. Atmos. Chem. Phys. 13, 1395–1410. https://doi.org/10.5194/acp-13-1395-2013.
Prudhomme, C., Reed, D., 1999. Mapping extreme rainfall in a mountainous region using geostatistical techniques: a case study in Scotland. Int. J. Climatol. 19, 1337–1356.
Raziei, T., Parehkar, A., 2021. Performance evaluation of NCEP/NCAR reanalysis blended with observation-based datasets for estimating reference evapotranspiration across Iran. Theor. Appl. Clim. 144, 885–903. https://doi.org/10.1007/s00704-021-03578-0.
Rolland, C., 2003. Spatial and seasonal variations of air temperature lapse rates in Alpine Regions. J. Clim. 16, 1032–1046.
S. Schimanke M. Ridal P. Le Moigne L. Berggren P. Undén R. Randriamampianina U. Andrea E. Bazile A. Bertelsen P. Brousseau P. Dahlgren L. Edvinsson A. El Said M. Glinton S. Hopsch L. Isaksson R. Mladek E. Olsson A. Verrelle Z.Q. Wang CERRA sub-daily regional reanalysis data for Europe on single levels from 1984 to present Copernic. Clim. Change Serv. (C3S) Clim. Data Store (CDS) 2021 doi: 10.24381/cds.622a565a.
Sabater, J. Muñoz ERA5-Land hourly data from 1981 to present Copernic. Clim. Change Serv. (C3S) Clim. Data Store 2019 doi: 10.24381/cds.e2161bac.
Soci, C., Bazile, E., Besson, F., Landelius, T., 2016. High-resolution precipitation reanalysis system for climatological purposes. Tellus A 68, 1–19. https://doi.org/10.3402/tellusa.v68.29879.
Srivastava, P.K., Islam, T., Gupta, M., Petropoulos, G., Dai, Q., 2015. WRF dynamical downscaling and bias correction schemes for NCEP estimated hydro-meteorological variables. Water Resour. Manag. 29, 2267–2284. https://doi.org/10.1007/s11269-015-0940-z.
Vanella, D., Intrigliolo, D.S., Consoli, S., Longo-Minnolo, G., Lizzio, G., Dumitrache, R.C., Mateescu, E., Deelstra, J., Ramírez-Cuesta, J.M., 2020. Comparing the use of past and forecast weather data for estimating reference evapotranspiration. Agric. Meteorol. 295, 108196 https://doi.org/10.1016/j.agrformet.2020.108196.
Vanella, D., Longo-Minnolo, G., Belfiore, O.R., Ramírez-Cuesta, J.M., Pappalardo, S., Consoli, S., D'Urso, G., Chirico, G.B., Coppola, A., Comegna, A., et al., 2022. Comparing the use of ERA5 reanalysis dataset and ground-based agrometeorological data under different climates and topography in Italy. J. Hydrol. Reg. Stud. 42, 101182 https://doi.org/10.1016/j.ejrh.2022.101182.
Yu, X., Qian, L., Wang, W., Huo, X., Hu, X., Wang, Y., 2023. Assessing and comparing reference evapotranspiration across different climatic regions of China using reanalysis products. Water 15, 2027. https://doi.org/10.3390/w15112027.
Zhao, P., He, Z., 2022. A first evaluation of ERA5-land reanalysis temperature product over the Chinese Qilian Mountains. Front. Earth Sci. 10, 907730 https://doi.org/10.3389/feart.2022.907730.